Analysis of Vascular Structure using Dual MDCT: Evaluation of 3 and 4 Dimensional Morphology of Vascular Structure and Analysis of Organic Blood Perfusion

Shoki Takahashi[*], Kei Takase, Yoshiaki Morita, and Tomonori Matsuura

* Professor
Department of Radiology, Graduate School of Medicine
E-mail: t-shoki@rad.med.tohoku.ac.jp

1. Abstract

We have performed medical care and analysis of various vascular diseases using 3 and 4 dimensional imaging using CT and MRI. Dual energy CT that has two X-ray sources with different tube voltage of 80 and 140 kV became available from 2007.   This newly developed machine enables characteristic diagnosis of vascular wall.   Furthermore, new bio-nano-imaging device such as dual energy CT, 3-Tesla MRI enables more detailed 3 and 4 dimensional analyses and functional analysis of vascular structure. In this report, we describe about our vascular analysis: 1. adrenal venous analysis, 2. preoperative vascular simulation of esophageal cancer, 3. dual energy MDCT analysis of the aorta, and 4. lung perfusion analysis.

Theme 1: Evaluation of adrenal venous structure and its anatomical variants using multi-detector row CT.

Introduction

Primary aldosteronism is the most common form of secondary hypertension, and its prevalence in hypertensive populations is estimated at approximately 10% [1,2]. Unilateral aldosterone-producing adenoma and bilateral idiopathic hyperaldosteronism are the two most common subtypes of primary aldosteronism, and distinguishing between them is critical for treatment planning. Adrenalectomy in patients with a unilateral aldosterone-producing adenoma mitigates hypertension, while hypertension due to bilateral idiopathic hyperaldosteronism is treated medically.   Adrenal venous sampling is an essential diagnostic step [6,7].

Multi-detector row CT (MDCT) could possibly guide adrenal venous sampling if it were capable of delineating the anatomy of the right adrenal vein (RAV). Although Daunt referred to the feasibility of identifying the RAV with MDCT [12], to our knowledge, a detailed analysis regarding visualizing the anatomy of the RAV with MDCT has never been made. We undertook this study to determine how frequently the RAV could be unequivocally identified on MDCT and what spectrum of anatomic variations was seen among the RAVs visualized.

Materials and Methods

The institutional review board approved this study; informed consent was not required for this retrospective study.

Patients
We performed a retrospective analysis of CT images from 104 consecutive patients

CT examination
Scans were obtained with the following parameters: 0.5 second per rotation, 1 mm collimation, and 14 mm/sec table increment (pitch, 7.0). Patients were requested to hold their breath for approximately 40 seconds during the scanning.

Before scanning was started, 100 mL of a contrast material containing 300 mg of iodine per milliliter was injected into an antecubital vein at a rate of 3.5 mL/sec.

Results

1. Degree of visualization of the RAV
The RAV was detected in 79 (76%) of 104 patients according to our identification criteria (Fig.1).

2. Relationship of the RAV to an accessory hepatic vein
The RAV and an accessory hepatic vein formed a common trunk before entering the IVC in 6 patients. In 7 patients, the RAV almost shared a common orifice with an accessory hepatic vein (9% of the 79 patients).

3. Location of the RAV orifice in relation to surrounding structures
The orifice was craniocaudally located between the level of T11 and L1 (Fig. 2). In 50 (69%) of the 73 patients, the RAV joined the IVC at the level ranging from the middle third of T12 to the superior third of L1. The transverse distance from the right margin of the vertebral bodies averaged 9.3 mm. As to the vertical relationship to the right renal vein, the RAV joined the IVC an average of 48 mm above the lower end of the orifice of that vein. Angle representing the position of the orifice along the circumference of the IVC ranged

from −7° to 71° (mean, 39°). The RAV joined the IVC in the right posterior quadrant in 97%.

4. Direction of the RAV at the branching portion from the IVC

The direction of the RAV from the IVC was posterior and rightward in 56 (77%) and posterior and leftward in 17 (23%) of the 73 patients.

The angle ranged from 30° to 136° (mean, 73°), and most patients showed a value between 50° and 90°. The direction of the RAV from the IVC was caudal in 65 (89%) and cranial in 8 (11%) of the 73 patients.

5. Length and diameter of the RAV

The length ranged from 1.2 to 8.6 mm (mean, 3.8 mm), and the diameter at the junction with the IVC ranged from 1.0 to 6.0 mm (mean, 1.7 mm).
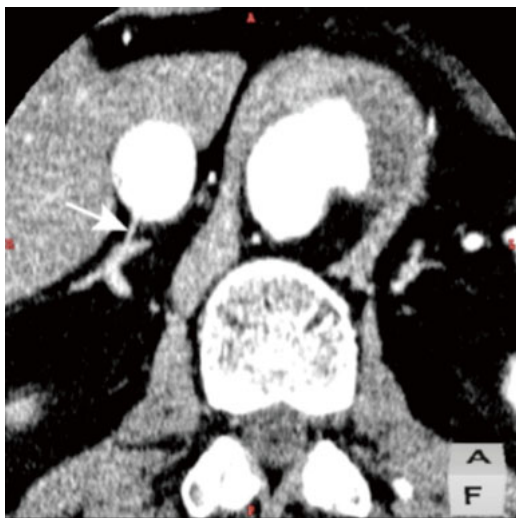

Fig. 1. A 56-year-old man with an aortic dissection. A para-axial multiplanar reconstruction (MPR) image shows excellent visualization of the right adrenal vein (RAV, arrow) running through the intervening adipose tissue to join the right posterior quadrant of the inferior vena cava. The length of the RAV was 8 mm.
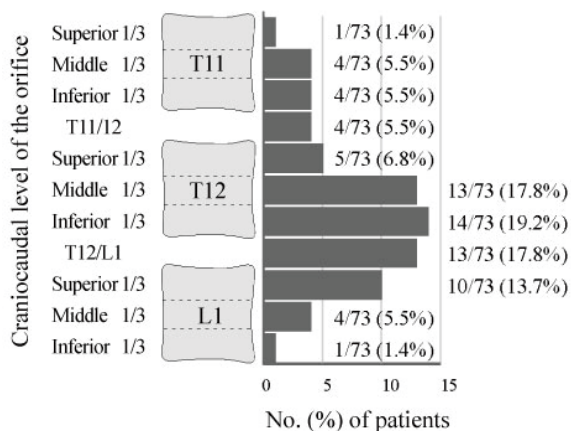

Fig. 2. The craniocaudal level of the right adrenal vein orifice in relation to the vertebrae. T11, T12 and L1 represent 11th and 12th thoracic and 1st lumbar vertebrae, respectively.
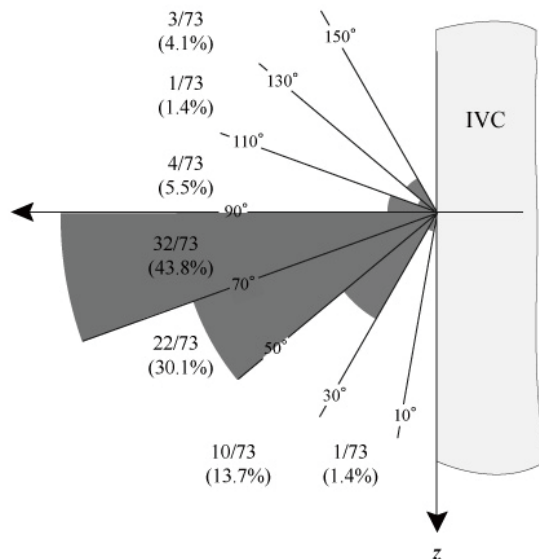

Fig. 3. The craniocaudal angle of the right adrenal vein with z-axis in the vertical plane. IVC = inferior nena cava.

Discussion

MDCT enabled the identification of the RAV in most patients. The enhanced structure of the RAV was easily detected in patients, especially when it was surrounded by abundant adipose tissue. In the cases in which the RAV was identified, the RAV anatomy including the position in relation to the IVC and surrounding structures was well evaluated. The results of our anatomical investigation using MDCT were generally concordant with the previous investigations by venography or autopsy.

In conclusion, MDCT enabled the identification of the RAV and delineation of its anatomy, including the position and relationship to the surrounding structures such as the IVC in a high percentage of patients. This preoperative information would help in the catheterization of the RAV for adrenal venous sampling.

94

Theme 2: Simulation of thoracoscopic esophageal surgery using MDCT and multiobject image analyzing function.

Introduction

Thoracoscopic surgery for esophageal cancer was developed as a minimally invasive surgery [5-7] that enables the operation to be performed through small wounds and ameliorates the postoperative decline in respiratory function compared to open surgery [8]. However, obtaining an entire view of the operative field is difficult using this approach. Moreover, the lack of tactual sensation and perspective during the thoracoscopic procedure makes it difficult for the surgeon to comprehend the three-dimensional (3-D) relationships of the mediastinal structures. Therefore, the vessels and organs in the mediastinum may occasionally suffer damage during the operation, which can lead to lethal complications.

In recent years, the development of technology, including MDCT and sophisticated workstations, has enabled preoperative 3-D simulation for various procedures such as laparoscopic gastric surgery, partial nephrectomy, and minimally invasive cardiac surgery [9-11]. The increasing use of endoscopic surgery is greatly contributing to the need for surgical simulation images.

The location and relationship of the lesion with underlying anatomical structures should be known with great accuracy before endoscopic surgery, as the incision and viewing field are small. Thoracoscopic surgery of esophageal cancer is a complicated procedure that requires precise anatomical recognition of thoracic vessels and organs, and accurate 3-D simulation images could provide preoperative information to make the surgery safer and more efficient without presenting serious complications. To our knowledge, however, no study has been published that clearly focuses on preoperative simulation images for performing thoracoscopic esophageal surgery.

In this report, we describe our CT protocol, the postprocessing on the workstation, and the methods for evaluating the preoperative 3-D CT simulation images for thoracoscopic surgery.

Procedure Details

1. The Process of Thoracoscopic Esophageal Surgery

Patients are placed in the left lateral position for thoracoscopic esophageal surgery at our institution. An endoscope is inserted through a (central) port placed in the right 4th intercostal space at the midaxillary line. The surgical instruments used in the actual procedure are inserted through five additional ports placed around the central port.

During the operation, the right lung is collapsed, which is induced by single lung ventilation. The collapsed right lung is compressed ventrally, thereby enabling observation of the mediastinum from the right side.

The azygos arch is first divided by mechanical instruments. The thoracic esophagus is then freed, and the mediastinal lymph nodes are dissected at the different levels of the mediastinum.

At the upper mediastinal level, the upper esophagus is freed from the trachea, and swollen paratracheal lymph nodes are dissected if present.

At the intermediate mediastinal level of the tracheal bifurcation and pulmonary hilum, the middle esophagus is freed from the surrounding structures (thoracic aorta and left bronchus) and swollen subcarinal lymph nodes are dissected. The surgeon may identify the bronchial arteries on both sides that must be preserved.

At the lower mediastinal level, the lower esophagus is freed from the surrounding structures (thoracic aorta and left atrium of the heart), and swollen posterior mediastinal lymph nodes are dissected.

After freeing the thoracic esophagus, the esophagus is removed by way of another separate abdominal incision that is also used for constructing an esophageal substitute made of autologous gastric tissue.

Surgeons must recognize the exact locations of swollen lymph nodes and the anatomical relationships of the mediastinal structures such as the vessels (e.g., aorta, subclavian artery and vein, bilateral bronchial arteries, azygos vein), trachea, and bones before performing thoracoscopic esophageal surgery to prevent an inadvertent injury during dissection of the lymph nodes and esophagus.

2. CT Scanning Protocol

Patients scheduled for thoracoscopic surgery of esophageal cancer undergo a dual phase post-contrast study by multi-detector CT (MDCT). Images are obtained using a 16-detector row CT (Aquilion; Toshiba Medical Company, Tokyo, Japan). A 20-gauge I.V. catheter is inserted from the left basilic vein. When a suitable basilic vein cannot be located, the right external jugular vein is used. A total of 100 ml of contrast material containing 350 mg iodine/ml is injected at a rate of 4.0 ml/s. Arterial and venous phase scanning are performed. In the arterial phase, the scan delay after the start of the contrast material injection is set by a bolus tracking method (Surestart; Toshiba). The region of interest (ROI) is positioned at the descending aorta, and the threshold for CT angiography is set at +100 HU. When the CT value reaches above the threshold, helical scanning is started automatically. Venous phase scanning follows 20 s after completion of the arterial phase scanning. The patients hold their breath for approximately 30–40 s during scanning with oxygen inhalation.

Scanning is performed with the following parameters: 0.5 s/rotation, 0.5-mm collimation, 15 mm/s table increment (helical pitch = 15), 120 kV, and 300 mA.

Axial slices are reconstructed with a 0.5-mm thickness at 0.5-mm intervals and transferred to a workstation (ZIO M900 QUADRA; ZIO Software, Tokyo, Japan).

3. The 3-D Images for Surgical Simulation

We use a workstation that features a "multi-volume function" for postprocessing that can separately generate different structures as multiple volume data; a maximum of eight different volumes can be generated and superimposed by this workstation. The workstation also has a "dual-phase fusion image" function that enables the superimposition of multiple volumes generated in different (arterial and venous) phases. For this purpose, however, the scan range and the parameters in the arterial and venous phases must be identical.

For the thoracoscopic simulation, we segment the surgical area into eight volumes as follows: (1) major vessels (aorta and its main branches, vena cava, brachiocephalic and subclavian veins, and pulmonary vessels); (2) bilateral bronchial arteries; (3) azygos vein; (4) bone; (5) trachea and lungs; (6) esophagus; (7) lymph nodes; and (8) skin. Among these structures, we generate the volume data for (1) the major arteries and veins from both the arterial and venous phases, (2) the bilateral bronchial arteries, (5) trachea and lungs, (6) esophagus, (7) lymph nodes, and (8) skin from the arterial phase, as well as (3) the azygos vein and (4) bone from the venous phase. The extraction of the bone volume is easier in the venous phase than in the arterial phase because the overlap of the densities between the bone and vascular volumes are smaller in the venous phase.
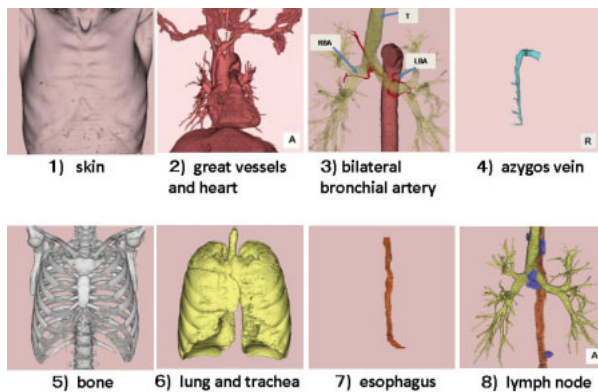

Fig. 4. Multivolume

3-A) Volumes of intrathoracic vessels

Thoracic 3-D CT angiography is reconstructed by setting a CT attenuation number threshold. It comprises major vessels (aorta and its main branches, vena cava,

brachiocephalic and subclavian veins, and pulmonary vessels), bilateral bronchial arteries, and the azygos vein. The right pulmonary vessels distal to the pulmonary hilum are removed from the images because the right lung is collapsed during the surgery by means of split ventilation.

3-B) Volumes of organs in the thorax

Multiple anatomical structures such as the skin, bone, lung, trachea and bronchi, esophagus, and lymph nodes are separately reconstructed and differently colored.

The bone volume is reconstructed by setting the lower limits of the CT attenuation number. The volumes of the trachea and lung are reconstructed by setting the upper limits of the CT attenuation number. The right bronchus distal to the pulmonary hilum and right lung are removed from the images. The volumes of the esophagus and swollen lymph nodes are also extracted by manually enclosing each target object on the original axial images. The skin volume is reconstructed by subtracting the volumes of the vessels and organs from the entire volume.

3-C) Fused 3-D simulation images (Fig. 5)

Finally, the volumes of the intrathoracic vessels and organs are fused together to show the relationships between all the anatomical structures in the thoracoscopic simulation images.

The superimposed 3-D volume rendering images are positioned as if the patient were supine with the head tilting toward the left side (simulating the positioning during surgery) and being viewed from the right lateral side.
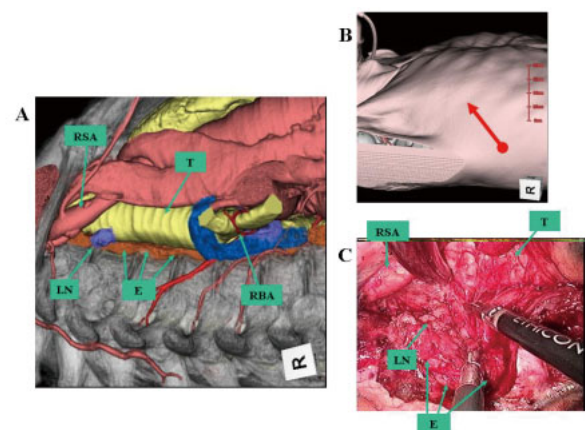

Fig. 5. Fused 3D simulation images
MDCT provides virtual endoscopic image simulating thoracoscopic image of the right thoracic cavity.

4. Virtual Thoracoscopy Technique

The radiologists and surgeons inspect the final fused 3-D simulation images and identify each anatomical

structure. The virtual endoscopy mode function of the workstation is used, which allows us to change the point of view by which we are looking at the thoracic cavity, as if we were observing through an actual thoracic endoscope. We call this process of observation the "Virtual thoracoscopy technique."

When we observe the 3-D simulation images, the structures that are to be resected during the operation such as the esophagus, lymph nodes, and azygos vein, can be removed on the virtual thoracoscopy as well. In addition, by changing the transparency of the volumes, the volume of interest that is behind volumes of other organs can be seen. For example, the lymph node along the left side of the esophagus at the paratracheal region can be recognized by increasing the transparency of the "tracheal volume."

We observe the simulated 3-D images in the following order: (4-A) insertion of the endoscope into the thoracic cavity, (4-B) observation at the upper mediastinal level, (4-C) observation at the intermediate mediastinal level of the tracheal bifurcation and pulmonary hilum, and (4-D) observation at the lower mediastinal level.

4-A) Insertion of the endoscope into the thoracic cavity (Fig. 6)

The point of view of the virtual endoscopy is first moved into the thoracic cavity from the right 4th intercostal space at the midaxillary line in the same way as the actual operation to view the right side of the mediastinum. After this observation, the surgeons might adjust the position of the ports.

4-B) Observation at the upper mediastinal level (Fig. 7)

At this level, the structures to be identified are the
- trachea, including checking the presence or absence of a tracheal diverticulum;
- upper esophagus;
- superior vena cava, right brachiocephalic vein, and subclavian vein;
- right brachiocephalic and subclavian artery;
- bones; and
- lymph nodes (paratracheal and paraesophageal).

These anatomical structures must be identified prior to dissection of the upper esophagus and lymph nodes to prevent injury of the surrounding vessels and trachea.

A tracheal diverticulum is rarely observed in the upper mediastinum as paratracheal air cysts communicating with the tracheal lumen [12]. If this structure exists in the upper mediastinum, the surgeons should pay careful attention to preventing injury of the diverticulum during paratracheal lymph node dissection. Thus, preoperative information about the presence of a tracheal diverticulum is extremely important .
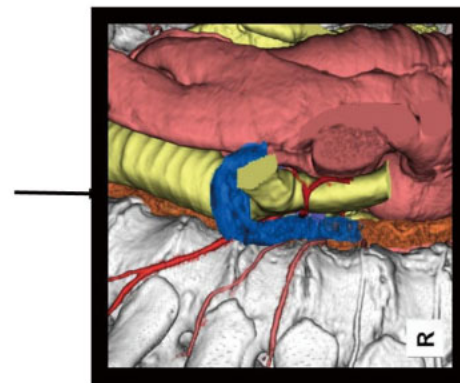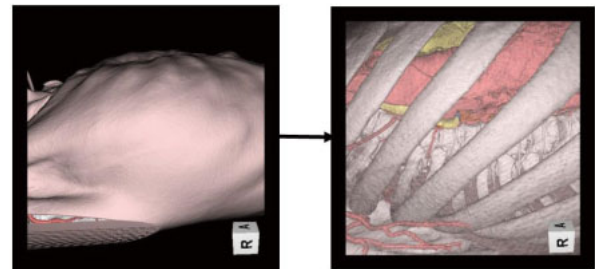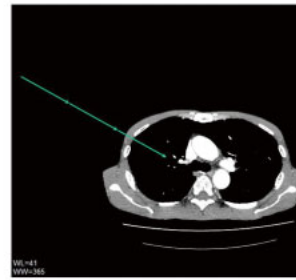

Fig. 6. Virtual thoracoscopy technique
The point of is inserted into the right thoracic cavity (green arrows). Firstly, surface of the skin is viewed from the right side of the body. Then, the organs in the thoracic cavity are seen through semitransparent skin. After the point of view is moved into the thoracic cavity, detailed structure of the thoracic cavity including great vessels, bronchial arteries, azygos, thorachea can be seen simulating thoracoscopic surgery.

4-C) Observation at the intermediate mediastinal level (the tracheal bifurcation and pulmonary hilum)

At this level, the structures to be identified are the
- tracheal bifurcation, bronchus;
- middle esophagus;
- thoracic aorta;
- bilateral bronchial arteries;
- superior vena cava, azygos vein;
- right pulmonary artery and vein;
- bones; and
- lymph nodes (subcarinal, main bronchus, and paraesophageal).

At this level, identification of the azygos vein and bilateral bronchial arteries is especially important , and because the azygos vein is divided during esophagectomy, its relationship with the surrounding structures should be checked .

The bronchial arteries are considered to vary in their origin, number, branching pattern, and anatomical course [13-21]. Therefore, these arteries can occasionally be damaged during surgery, possibly leading to a complication such as tracheal necrosis and/or uncontrollable bleeding. Their anatomy must be assessed preoperatively to avoid injury when the esophagus is being freed and the tracheal bifurcation and middle paraesophageal lymph nodes are being dissected . In addition to the right bronchial arteries, the left bronchial arteries are also observable by increasing the transparency of the bronchus. Because the left bronchial arteries are difficult to detect during surgery, this is very useful preoperative information for avoiding damage to these arteries.

4-D) Observation at the lower mediastinal level

At this level, the structures to be identified are the
- lower esophagus,
- descending aorta,
- heart,
- inferior vena cava,
- bones, and
- lymph nodes (paraesophageal and posterior mediastinal).

These anatomical structures must be identified prior to dissection of the lower esophagus and lymph nodes to prevent injury to the surrounding vessels and heart.
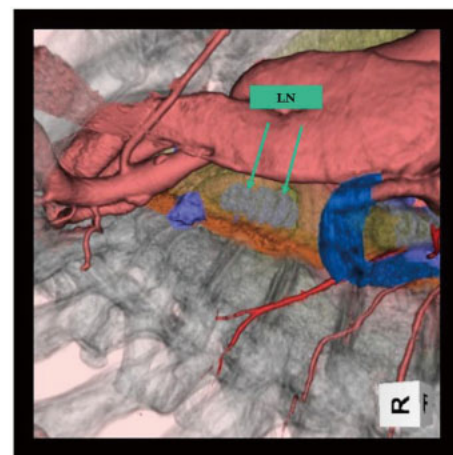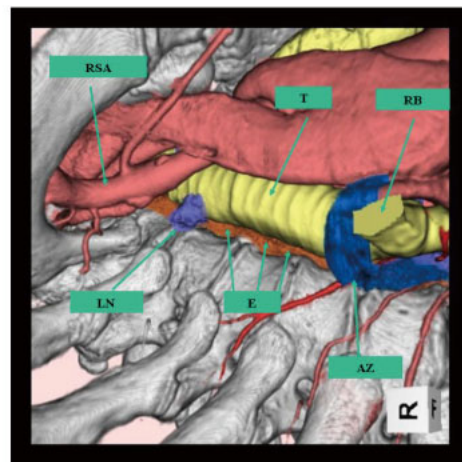

Fig. 7. Virtual thoracoscopy technique
(Upper mediastinal view simulating the first step of thoracoscopic surgery)
Right subclavian artery (RSA), trachea (T), right main bronchus (RB), Esophagus (E), azygos vein (AZ), and suspected metastatic lymphnodes (LN) are well visualized.
Green arrow shows the line of vision of the virtual endoscopy.

5. The Use of the Simulation Images by Surgeons for Thoracoscopic Surgery

Information obtained during virtual thoracoscopy is saved as key image files as well as video files, which can be viewed by the surgeons both before and during the surgery.

The virtual thoracoscopy technique provides anatomical information on the mediastinal structures (e.g., vessels, trachea, and bone) and swollen lymph nodes around the esophagus at each mediastinal level. The surgeons should preoperatively check the following: the anatomical relationship between the esophagus and adjoining mediastinal organs; exact location of swollen lymph nodes, including their relationships to surrounding organs; existence of an anomaly of the great vessels or trachea; elongation of the aorta or right subclavian artery; and the degree of vertebral deformity.

At the intermediate mediastinal level with the tracheal bifurcation and pulmonary hilum, information on both bronchial arteries is especially important. The surgeons identify their number, branching pattern, and anatomical course before surgery. In most cases, the right bronchial artery arises from the intercostobronchial artery and runs along the right side of the esophagus . In contrast, the left bronchial artery mostly arises directly from the thoracic aorta and runs along the left side of the esophagus . Both bronchial arteries usually run dorsal to the trachea . However, variation is frequent in the bronchial arteries. For example, we experienced a common trunk of the bronchial arteries on both sides that descended along the left side of the esophagus and ventral to the trachea–bronchi . In this case, preoperative anatomical information helped the surgeons preserve the bronchial arteries during dissection of the subcarinal lymph nodes and freeing of the middle esophagus.

6. Limitation and Future Prospectives

As described above, bronchial arteries are important structures in performing thoracoscopic esophageal surgery. Thoracic duct and nerves (Vagal nerve, recurrent nerve etc.) are also important structures related to surgical procedure and post operative complications. Those structures are difficult to evaluate by MDCT because of low contrast resolution between them and surrounding soft tissue. MRI, which has better contrast resolution than CT, may enables visualization of these structures using various scanning sequences. Some reports refer to visualization of thoracic duct by MRI [22].

In the near future, it will become possible to render fusion image of multi-modality images such as MDCT, MRI and PET. Then we can image vascular structures, bones, thorachea and lung, esophagus, tumor, thoracic duct, nerves, and positive lymph nodes in a fused 3D-simulation image.

7. Conclusions

Virtual CT thoracoscopy allows clear visualization of the anatomy of intrathoracic structures, and surgeons can simulate thoracoscopic surgery as if they were observing the surgery through an actual thoracic endoscope. This type of preoperative information will permit surgeons to perform thoracoscopic esophageal surgery both efficiently and safely and to improve the surgical results by allowing them to recognize the important surrounding structures, correctly dissect the lymph nodes, and preserve the bronchial arteries.

Theme 3: Cardiac imaging by Dual Source MDCT

4.1. Introduction
MDCT imaging of the cardiac structure has rapidly progressed. Because of the limitation of the temporal resolution, it has been difficult to evaluate coronary artery of the patients with high heart beat. We have installed dual source CT that has high temporal resolution of 83msec, which enables 4-dimensional imaging with high spatial and temporal resolution. We are now utilizing this newly developed machine.

4.2. Materials and methods
Diseases : coronary artery, valvular diseases, congenital heart disease, arrythmia
Image analysis : coronary analysis, myocardial perfusion, 4-dimensional cardiac functional analysis, Simulation of arrhythmia ablation.

4.3. Result
Systolic phase images were significantly improved using dual source CT compared to single source CT due to advancement of temporal resolution. Therefore, accuracy of cardiac functional analysis and success rate of optimal coronary visualization improved. (Fig. 8. left side).

We are now performing cardiac atrial functional analysis that reflects effectiveness of ablation therapy for arrhythmia. Four-dimensional analysis for evaluation of cardiac valvular disease became available. （Fig. 8. right side, Fig. 9,10）
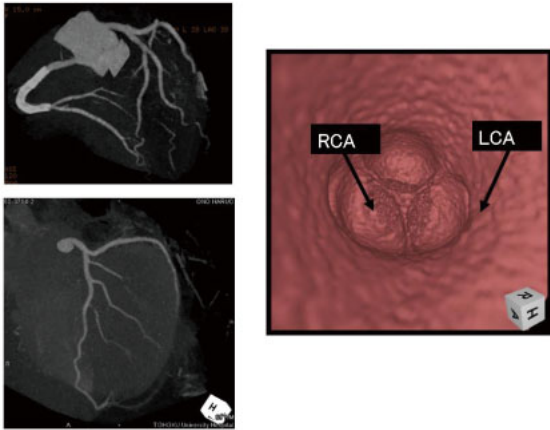
Fig. 8. Left side: coronary CT using dual source CT. Maximal intensity projection image eliminating cardiac ventricles and atria (angiographic view).
Right side: Virtual endoscopic image of aortic valve. Three coronary cusps can be well visualized.
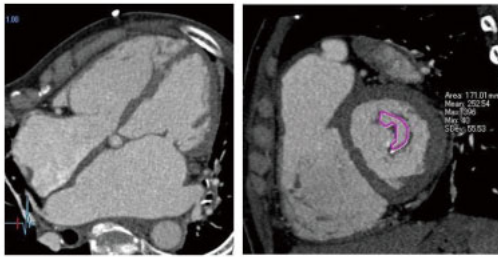

Fig. 9. ECG-gated diastoric phase image of the patient with mitral stenosis. Restriction of the mitral valve opening is well visualized. Short axial multiplanar reformat image of the mitral valve arrows measurement of mitral valve area.
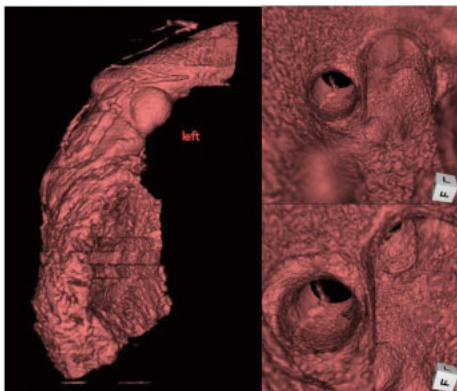

Fig. 10. Left side: right ventricle viewed from left side.
Right side: Virtual endoscopic image of the right ventricle.
Catheter ablation therapy for arrhythmia is scheduled for the patient. Origin of the arrhythmia is thought to be located in the right ventricular outflow. Virtual endoscopy images help understand the manipulation of the catheter.

Theme 4: Imaging using Dual Energy CT Aorta, Arteriosclerosis, and Pulmonary perfusion

5.1. Introduction

Dual source/energy CT utilizes the difference of absorption characteristics between biologic objects, enabling new radiological diagnosis such as automatic segmentation of the structures, imaging of iodine distribution and so on. We apply this new method to diagnosis of vascular disease making studies on arteriosclerosis obliterance, 3-D rendering, and evaluation of lung perfusion.

5.2. Materials and method:

Patients: Arteriosclerosis obliterance, aortic aneurysm, pulmonary thromboembolism
Method:
Three dimensional CT angiography using dual energy tubes of 80 kV and 140 kV. Evaluation of perfused blood volume of the lung.

5.3. Result

Dual Energy CT enables automatic elimination of the bony structure by analyzing dual energy factor. (Fig. 11)

We are now performing study about CT evaluation of diseases with decreased pulmonary perfusion. Pulmonary perfusion image superimposed with anatomical image is expected to enable high resolution functional analysis of pulmonary vascular diseases.

Fig. 11. Dual Energy CT of the aorta and iliac arteries. Bony structures are mostly eliminated automatically.
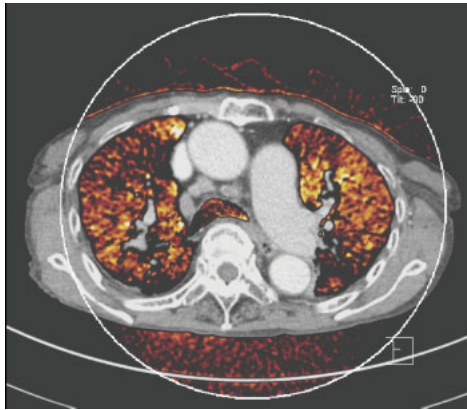
Fig. 12. Dual energy CT of pulmonary thromboembolism. Thrombus (arrowhead) is visualized in the lower branch of the right pulmonary artery in anatomical CT image. Hypoperfusion area can be evaluated by perfusion image as color defect.

Reference

[1] Mulatero P, Stowasser M, and Loh KC. Increased diagnosis of primary aldosteronism, including surgically correctable forms, in centers from five continents. *J Clin Endocrinol Metab* **89**, 1045-1050, 2004.

[2] Doppman JL, Gill Jr JR, and Miller DL. Distinction between hyperaldosteronism due to bilateral hyperplasia and unilateral aldosteronoma: reliability of CT. *Radiology* **184**, 677-682, 1992.

[3] Radin DR, Manoogian C, and Nadler JL. Diagnosis of primary hyperaldosteronism: importance of correlating CT findings with endocrinologic studies. *AJR Am J Roentgenol* **158**, 553-557, 1992.

[4] Magill SB, Raff H, Shaker JL, and et al. Comparison of adrenal vein sampling and computed tomography in the differentiation of primary aldosteronism. *J Clin Endocrinol Metab* **86**, 1066-1071, 2001.

[5] Morita Y, Takase K, Yamada T, Sato A, Higano S, Takahashi S, and Ichikawa H. Virtual CT thoracoscopy: preoperative simulation for thoracoscopic surgery of esophageal cancer. *Abdom Imaging*, 2007 (Epub ahead of print).

[6] Yamamoto S, Kawahara K, Maekawa T, Shiraishi T, and Shirakusa T. Minimally invasive esophagectomy for stage I and II esophageal cancer. *Ann Thorac Surg* **80**, 2070-5, 2005.

[7] Akaishi T, Kaneda I, Higuchi N, Kuriya Y, Kuramoto J, Toyoda T, and Wakabayashi A. Thoracoscopic en bloc total esophagectomy with radical mediastinal lymphadenectomy. *J Thorac Cardiovasc Surg* **112**, 1533-1540, discussion 1540-1, 1996.

[8] Osugi H, Takemura M, Lee S, Nishikawa T, Fukuhara K, Iwasaki H, and Higashino M. Thoracoscopic esophagectomy for intrathoracic esophageal cancer. *Ann Thorac Cardiovasc Surg*, Review **11**, 221-227, 2005.

[9] Miyazaki S and Satomi S. Thoracoscopic esophageal surgery – current status and limitations. *Rinsho-Geka* **57**, 1347-1352, 2002 (in Japanese).

[10] Pramesh CS, Mistry RC, Sharma S, Pantvaidya GH, and Raina S. Bronchial artery preservation during transthoracic esophagectomy. *J Surg Oncol* **85**, 202-203, 2004.

[11] Kawanishi T and Chiba S. Anatomy of bronchial artery. *Hirosaki-Igaku* **33**, 386-403, 1981 (in Japanese).

[12] Takahashi D. Anatomy of bronchial artery and its clinical impact. *Hirosaki-Igaku* **42**, 230-242, 1990 (in Japanese).

[13] Matsuki M, Kani H, Tatsugami F, Yoshikawa S, Narabayashi I, Lee SW, Shinohara H, Nomura E, and Tanigawa N. Preoperative assessment of vascular anatomy around the stomach by 3D imaging using MDCT before laparoscopy-assisted gastrectomy. *AJR Jul* **183**, 145-51, 2004.

[14] Wunderlich H, Reichelt O, Schubert R, Zermann DH, and Schubert J. Preoperative simulation of partial nephrectomy with three-dimensional computed tomography. *BJU Int* **86**, 777-781, 2000.

[15] Sawamura Y, Takase K, Kikuchi S, and Ito T. Multislice helical computed tomography for minimally invasive cardiac surgery. *Ann Thorac Surg* **71**, 1707, 2001.

[16] Kobayashi K, Shibata Y, Yoneda K, and Matsui O. Visualization of normal bronchial artery by 16-detector raw MDCT. *Rinsho-Houshasen* **49**, 109-114, 2004 (in Japanese).

[17] Goo JM, Im JG, Ahn JM, Moon WK, Chung JW, Park JH, Seo JB, and Han MC. Right paratracheal air cysts in the thoracic inlet: clinical and radiologic significance. *AJR Am J Roentgenol* **173**, 65-70, 1999.

[18] Remy-Jardin M, Bouaziz N, Dumont P, Brillet PY, Bruzzi J, and Remy J. Bronchial and nonbronchial systemic arteries at multi-detector row CT angiography: comparison with conventional angiography. *Radiology* **233**, 741-749, 2004.

[19] Cuschieri A, Shimi S, and Banting S. Endoscopic oesophagectomy through a right thoracoscopic approach. *J Roy Coll Surg Ed* **37**, 7-11, 1992.

[20] Mori K. The mediastinal courses of the bronchial arteries: helical CT evaluation. *Nippon Igaku Hoshasen Gakkai Zasshi* **61**,156-162, 2001.

[21] Murayama S, Hashiguchi N, Murakami J, Sakai S, Matsumoto S, Mizushima A, Hasuo K, and Masuda K. Helical CT imaging of bronchial arteries with curved reformation technique in comparison with selective bronchial arteriography: preliminary report. *J Comput Assist Tomogr* **20**, 749-755, 1996.

[22] Matsushima S, Ichiba N, Hayashi D, and Fukuda K. Nonenhanced magnetic resonance lymphoductography: visualization of lymphatic system of the trunk on 3-dimensional heavily T2-weighted image with 2-dimensional prospective acquisition and correction. *J Comput Assist Tomogr* **31**, 299-302, 2007.

[23] Hayashi S and Miyazaki M. Thoracic duct: visualization at nonenhanced MR lymphography--initial experience. *Radiology* **212**, 598-60, 1999.